International Journal of Steel Structures
June 2011, Vol 11, No 2, 145-155
DOI 10.1007/s13296-011-2004-4

International Journal of
STEEL
STRUCTURES
www.springer.com/journal/13296

Temperature-induced Variations of Measured Modal Frequencies of Steel Box Girder for a Long-span Suspension Bridge

YouLiang Ding* and AiQun Li

Key Laboratory of Concrete and Prestressed Concrete Structures of Ministry of Education, Southeast University, Nanjing, Jiangsu Province, 210096, China

Abstract

This paper addresses the temperature-induced variations of measured modal frequencies of steel box girder for a suspension bridge using long-tem monitoring data. The output-only modal frequency identification of the bridge is effectively carried out using the Iterative Windowed Curve-fitting Method (IWCM) in the frequency-domain. The daily and seasonal correlations of frequency-temperature are investigated in detail and the analysis results reveal that: (i) the identified modal frequencies using IWCM provide an effective indication for changes of the bridge due to the ambient temperature variations; (ii) temperature is the critical source causing modal variability, and there is an overall decrease in modal frequency with temperature for all the identified modes; (iii) the random variations in measured modal frequencies mainly arise from the identification algorithm due to the nonstationary loadings, which can be effectively eliminated using multi-sample averaging technique; (iv) the daily averaged modal frequencies of vibration modes have remarkable seasonal correlations with the daily averaged temperature and the seasonal correlation models of frequency-temperature are suitable for structural damage warning if future seasonal correlation models deviate from these normal models.

Keywords: structural health monitoring, modal frequency, temperature effect, steel box girder, suspension bridge

1. Introduction

Over the past several decades, a significant research effort has focused on the health monitoring and condition assessment for long-span bridges (Doebling *et al*., 1998; Ko and Ni, 2005; Hsieh *et al*., 2006; Han *et al*., 2010). How to explain the health condition of the bridge structure according to the collected structural responses remains a great challenge in the civil engineering community. It is well known that bridge structures are subject to varying environmental conditions such as traffic loadings and environmental temperature. These environmental effects will cause changes in the structural damage detection parameters which may mask the changes caused by structural damage. Therefore, for reliable performance of structural health monitoring technique for long-span bridges, it is of paramount importance to characterize normal variability of damage detection parameters due to environmental effects and discriminate such normal variability from abnormal changes in damage detection parameters caused by structural damage (Ni *et al.*, 2005; Ding *et al*., 2008a; Lee *et al*., 2010).

Considerable research efforts have been devoted to investigating the influences of environmental conditions on modal frequencies of bridges. Most of these investigations have indicated that temperature is the most significant environmental effect affecting bridge modal properties (Abdel Wahab and De Roeck, 1997; Cornwell *et al*., 1999; Sohn *et al*., 1999; Peeters and De Roeck, 2001; Ni *et al*., 2005; Hua *et al*., 2007; Ni *et al*., 2009; Zhou *et al*., 2010). For instance, Abdel Wahab and De Roeck (1997) conducted two dynamic tests for a prestressed concrete bridge in spring and winter respectively, and observed an increase of 4~5% in modal frequencies with the decrease in temperature. Cornwell *et al*. (1999) observed the variability of modal frequencies by up to 6% over a 24-hour period on the Alamosa Canyon Bridge.

It should be noted that most of these studies observed the temperature-induced variations in measured modal frequencies. However, the modal variability induced by temperature was not systematically evaluated with regard to the daily and seasonal correlations. And it is more important that most studies did not take into consideration the measurement errors arising from the modal identification

Note.-Discussion open until November 1, 2011. This manuscript for this paper was submitted for review and possible publication on January 20, 2010; approved on May 9, 2011.

*Corresponding author
Tel: +86-25-8379-0921; Fax: +86-25-8379-0921
E-mail: civilding@yahoo.com.cn

Figure 1. View of the Runyang Suspension Bridge.

algorithm. For instance, Ni *et al*. (2007) observed that the normal environmental change of Ting Kau Bridge accounts for relative variation in modal frequencies from 3.22 to 15.07% for the first ten modes. Using the formulated frequency-temperature correlation models, the relative variation of the normalized frequencies after removing the temperature effect was reduced to range from 1.61 to 7.87%. In their studies the correlation between frequency and wind speed is very weak and the wind effect on the modal frequencies is of no significance. Thus, one possible reason for the considerable variations in the normalized frequencies after removing the temperature effect is that the measurement errors induced by the modal identification algorithm are significant. However, relevant works are seldom reported.

Based on the aforementioned motivation, the objective of this paper is to quantify the modal variability of long-span bridges induced by temperature and identification algorithm. First, the output-only modal frequency identification of the bridge is effectively carried out using the Iterative Windowed Curve-fitting Method (IWCM) in the frequency-domain. Then the daily and seasonal temperature-frequency correlations are formulated for each vibration mode to investigate the effect of temperature and identification algorithm. The feasibility of the proposed strategy is demonstrated using 215 days of health monitoring data obtained on the Runyang Suspension Bridge.

2. Structural Health Monitoring of Runyang Suspension Bridge

The subject of this study is Runyang Suspension Bridge shown in Fig. 1, which is a single-span steel suspension bridge with the main span 1,490 m. The aerodynamically shaped closed box steel girder is 36.3 m wide and 3.0 m high shown in Fig. 2. The health monitoring system for the Runyang Suspension Bridge has been established to real-time monitor the responses of the bridge under the various kinds of environment actions and mobile loads by application of modern techniques in sensing, testing, computing and network communications (Ding *et al*., 2008a).

As for the vibration monitoring of steel box girder of Runyang Suspension Bridge, a total of 27 uni-axial servo type accelerometers were installed at nine sections of the bridge deck to measure dynamic characteristics of the bridge as shown in Fig. 3. The nine sections are equidistantly located in the main span. In each deck section one lateral accelerometer directly recorded the lateral response and the vertical acceleration of the deck section was obtained by averaging the accelerations measured by the two vertical accelerometers located in the upriver and downriver cross sections, respectively. As for the temperature monitoring, a total of 40 temperature sensors were installed at five sections (Sec. 1, Sec. 2, Sec. 3, Sec. 4 and Sec. 9). The 8 temperature sensors (C1~C8) at each section are shown in Fig. 2, which can effectively measures the global temperature of the girder. The measurements were acquired at sampling rates of 1 and 20 Hz for temperature and acceleration, respectively.

3. Identification of Modal Frequencies

In order to provide an accurate and reliable evaluation

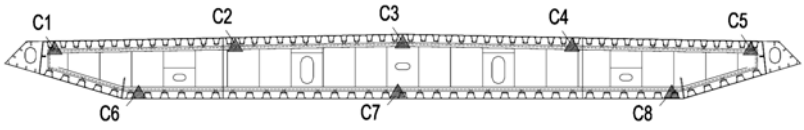

Figure 2. Section of steel box girder.

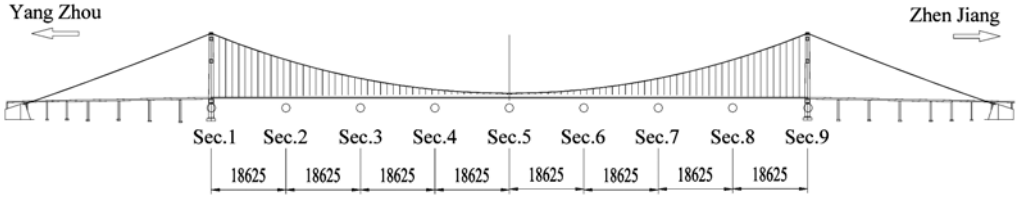

Figure 3. Layout of ambient vibration monitoring (Units: cm).

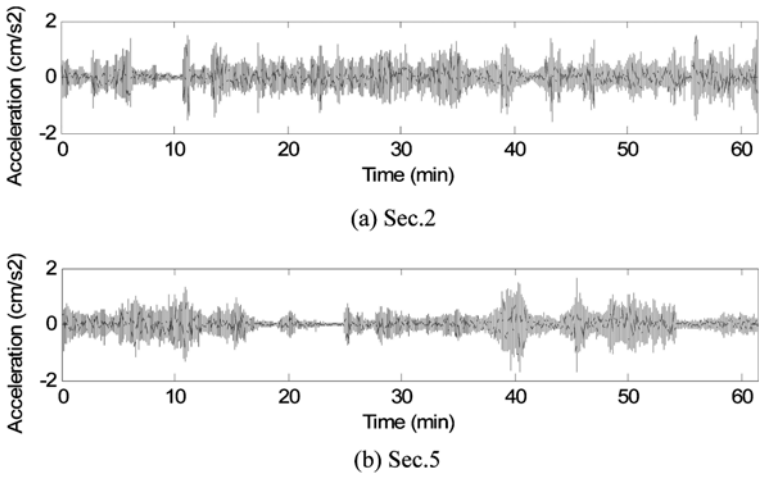

Figure 4. Vertical acceleration time histories of the bridge deck.

of the real dynamic characteristics of the Runyang Suspension Bridge, long-term field ambient testing was carried out from January to October of the year 2006. During this period, sufficient variations in ambient temperature were experienced for any trends in modal parameters to be identified.

In this study, the peak picking (PP) method in the frequency domain was used for the identification of modal frequencies of Runyang Suspension Bridge. In the PP method, the identified natural frequencies are simply obtained from the observation of the peaks on the graphs of the auto power spectral densities (PSDs) of the output-only data (Ren and Peng, 2005, Ding *et al*., 2008b). In order to overcome the shortcomings of the PP method such as limited frequency resolutions, the Iterative Windowed Curve-fitting Method (IWCM) is further used to improve the modal frequency estimations. IWCM is a frequency domain method, based on the curve fitting of Power Spectral Densities (PSDs), but modified to deal with spectral bias errors. Bias errors are a significant problem in conventional frequency domain methods, causing attenuation of values around spectral peaks in the PSD. This arises from the finite length of data segments used for the Fast Fourier Transform (FFT) estimation of the PSD. The key to IWCM is that it modifies the modal peaks of the theoretical PSD, to account for the bias, before it is fitted to the measured PSD. This is done by applying the same window function used on the measured data, in the time domain, to the theoretical spectral peaks, in the frequency domain, thus improving the modal frequency estimates. Details of IWCM are given in Ref. (Macdonald, 2000). In this study, the vertical accelerations of the bridge deck are employed for the modal analysis.

Figure 4 illustrates the vertical acceleration time histories of the bridge deck at the Sec. 5 and Sec. 2 shown in Fig. 3. It can be observed that the measured dynamic responses present the nonstationary characteristics due to the ambient loadings. In this study, per 10-min recorded data are used for PSD analysis. Before the PSD analysis is performed, the measured 10-min data are first detrended, which enables the removal of the DC-components that may badly influence the identification results. This was accomplished by subtracting the mean values calculated over the 10-min duration of each measurement (Ren *et al*., 2007). A sampling frequency of 20 Hz on site results in a frequency range from 0 to 10 Hz. For Runyang Suspension Bridge, however, the frequency range of interest lies between 0 and 2.0 Hz, covering the most important frequencies in the vertical directions. So a resampling of the raw measurement data is also necessary. A resampling and filtering from 20 to 4 Hz is the same as decimating (=low-pass filtering and resampling at a lower rate) 5 times which results in 12000/5=2400 data points per 10 minutes.

Figure 5 shows the measured normalized PSDs of deck acceleration responses and IWCM curve-fits to vertical deck PSDs. The good fits suggest that the identified modes describe the dynamic behavior of the structure well. As shown in Fig. 5, the peaks of the PSD plots clearly indicate the modal frequencies of the bridge. However, due to the limited measured sections, the analysis results of mode shapes are not satisfactory. Thus, in order to verify the identified modal frequencies, the previously obtained dynamic properties from the ambient vibration test conducted just prior to the opening of the bridge are further used (Ni *et al*., 2005), because in that vibration test 47 sections are installed accelerometers to obtain both modal frequencies and mode shapes, which are the basis for the proper determination of modal frequencies from the measured PSD plots such as Fig. 5.

Figure 6 shows the identified frequency sequences in a typical day for the Runyang Suspension Bridge using the IWCM. On the whole, the measured modal frequencies have the minimum approximately at 2:00 PM in the afternoon and reached to the maximum approximately at 6:00 AM in the wee hours. Therefore, the measured

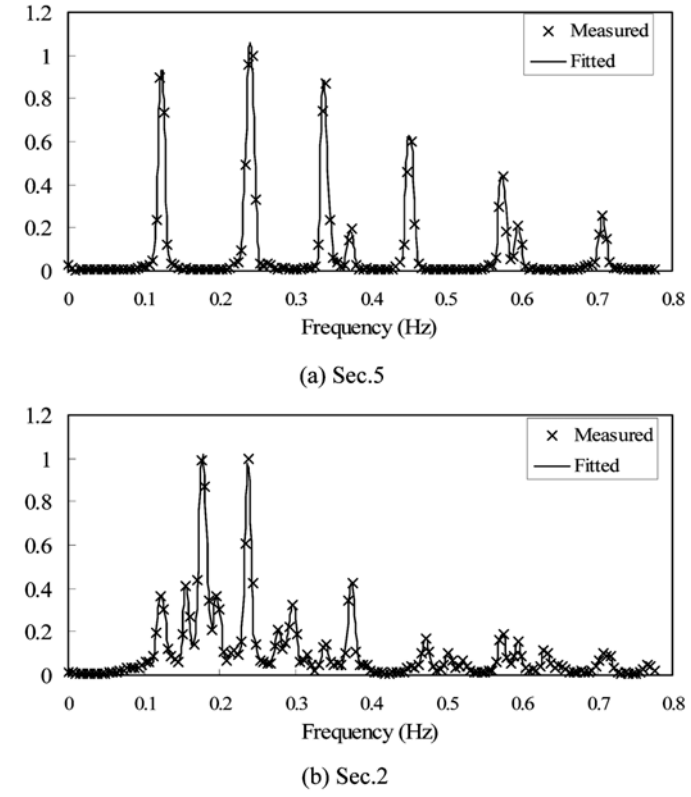

Figure 5. Typical curve-fit results of normalized PSD of vertical deck acceleration.

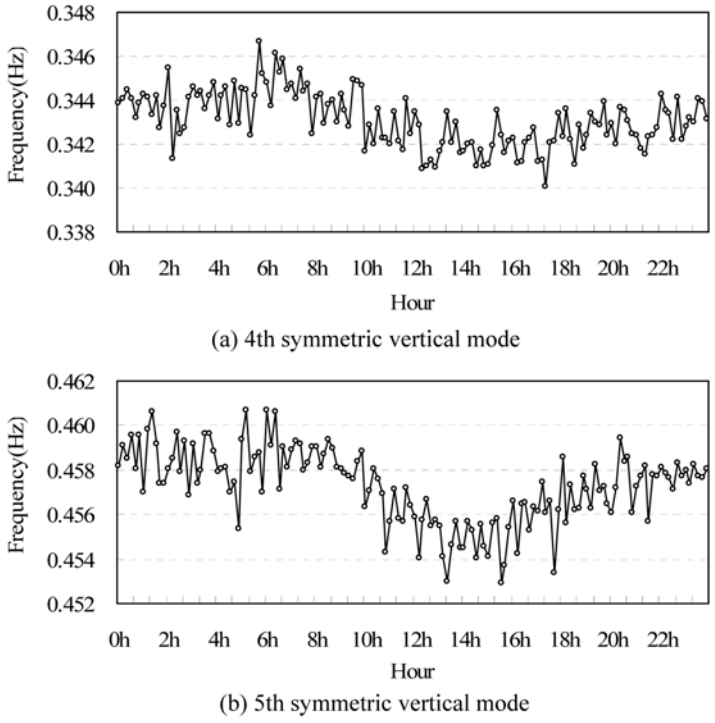

Figure 6. Measured frequency sequences using IWCM.

modal frequencies can effectively reflect the fluctuation characteristics of ambient temperature in one day. As for the comparisons, Fig. 7 gives the identification results using the conventional PP method. It can been seen that due to the limited frequency resolutions the identified modal frequency sequences without using IWCM fails to

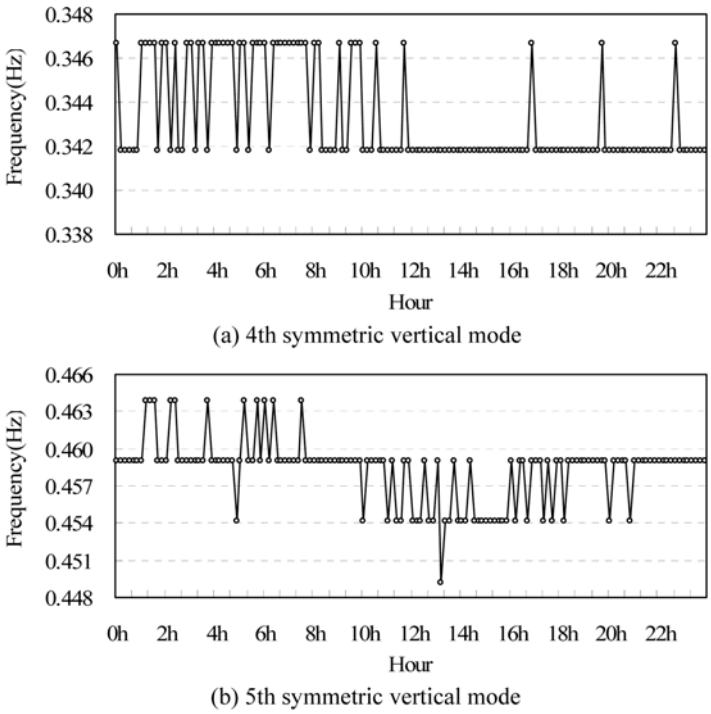

Figure 7. Measured frequency sequences using conventional PP method.

reflect the influence of daily temperature variations. Thus, the identified modal frequencies using IWCM provide an effective indication for changes of the bridge due to the ambient temperature variations. It should be noted that before using IWCM, it is necessary to pick up the peaks on the graphs of the PSDs for the frequency identification. For identified peaks using PP method, the usage of IWCM is to improve the modal frequency identification. It is usually observed that the PP method in the frequency domain cannot identify all important mode shapes for such a large bridge (Ren *et al*., 2007). Thus, the IWCM can only be used to overcome the shortcoming of PP method with limited frequency resolutions and cannot be used to obtain complete modal information. In addition, from Fig. 6 it can be observed that the influences of ambient loadings on the measured frequencies present instantaneous changes because the modal identification algorithm in the frequency domain assumes stationarity of loading and hence response. However, the measured dynamic responses of the bridge were rejected for statistically meaningful stationarity tests. Hence, the modal frequency variation induced by the modal identification algorithm is mainly random variations due to nonstationary ambient loadings.

4. Temperature-induced Variations of Modal Frequencies

4.1. Daily correlation analysis of temperature-frequency

The 215-day acceleration measurement data (from January to October of the year 2006), after removing those likely to be abnormal are used in this study. In order to exclude the influence of strong winds and extreme traffic loadings on the identified modal frequencies, the acceleration measurement data are further selected under weak wind and normal traffic conditions. Thus, the vertical acceleration responses are selected at 1-hour intervals when hourly-average wind speed is less than 2 m/s (Ni *et al*., 2007) and the root mean square (RMS) of the vertical acceleration responses calculated in the frequency band of 0-4 Hz is less than 2.5 cm/s^2 (Zhang *et al*., 2002).

With the selected acceleration measurement data, the modal frequencies of the 6 vibration modes of Runyang Suspension Bridge were identified at 10-min intervals, respectively. There are totally 17280 measured samples of modal frequencies. Table 1 summarizes the statistical information of measured modal frequencies from 215-day data in the year 2006 for Runyang Suspension Bridge. Figure 8 plots the values of modal frequencies versus temperature with regard to different vibration modes, in which the temperature data from all sensors were averaged to a value as the representative temperature of the bridge deck. For all the vibration modes, an overall decrease in modal frequency is observed with the increase in temperature of the bridge. And the measured modal frequencies of higher vibration modes are more sensitive to ambient temperatures. However, it is obvious that the measurement points in Fig. 8 are too dispersed to be an effective description of the correlation of frequency-temperature, implying that the influence of nonstationary

Table 1. Statistics of measured modal frequencies of Runyang Suspension Bridge

Mode No.	Nature of mode	Maximum (Hz)	Minimum (Hz)	Average (Hz)	Relative variation (%)
1	1st symmetric vertical mode	0.1249	0.1219	0.1236	2.4610
2	2nd anti-symmetric vertical mode	0.1823	0.1775	0.1797	2.7042
3	3rd anti-symmetric vertical mode	0.2829	0.2766	0.2791	2.2777
4	4th symmetric vertical mode	0.3468	0.3381	0.3408	2.5732
5	4th anti-symmetric vertical mode	0.3855	0.3742	0.3784	3.0198
6	5th symmetric vertical mode	0.4618	0.4500	0.4536	2.6222

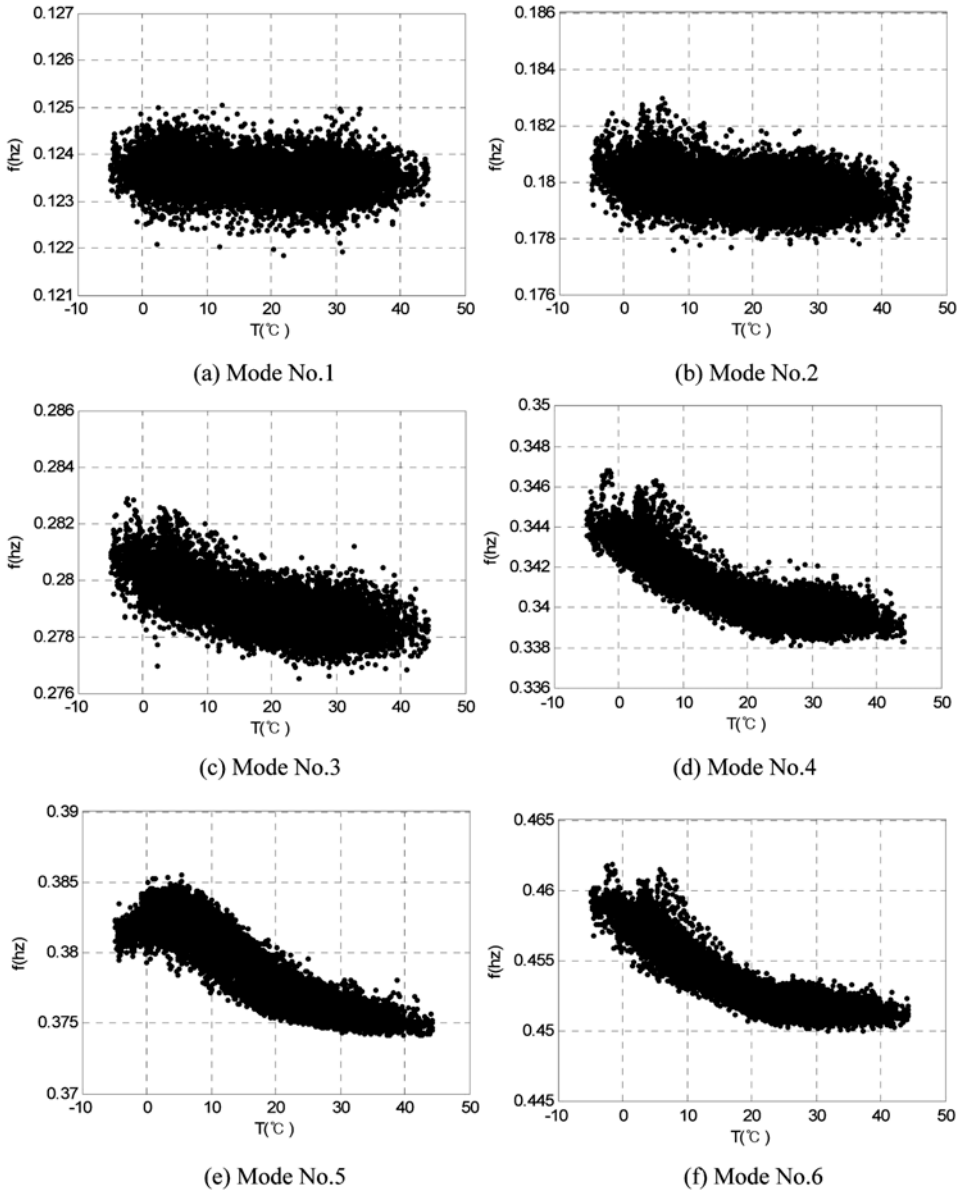

Figure 8. Daily correlations of frequency-temperature.

loading on the identification of modal frequencies is significant.

4.2. Seasonal correlation analysis of temperature-frequency

The seasonal correlation analysis is further applied to eliminate the random variations due to nonstationary loadings, namely using the daily averaged values to construct the seasonal relationship between frequency and temperature. In Fig. 9 the daily averaged frequency-temperature scatter diagrams of Runyang Suspension Bridge are presented. It can be shown that daily averaged

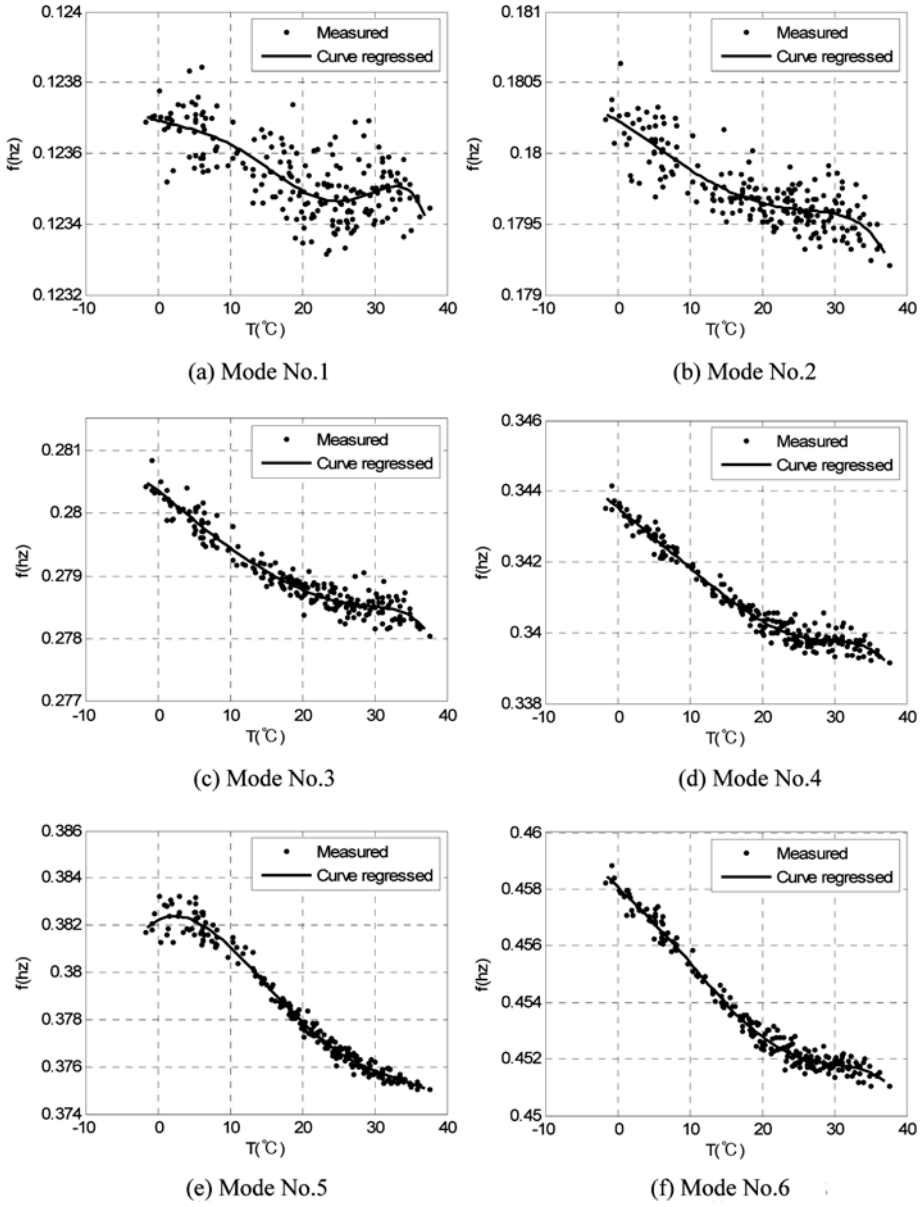

Figure 9. Seasonal correlations of frequency-temperature.

modal frequencies of vibration modes have remarkable seasonal correlation with the daily averaged temperature. Table 2 summarizes the statistical information of daily averaged modal frequencies from 215-day data in the year 2006. It can be observed that the maximum and averaged relative variations for Runyang Suspension Bridge reduced from 3.0198 and 2.6097% to 2.1322 and 1.2377%. Thus, the daily averaged frequencies using multi-sample averaging technique can effectively eliminate the random variations rising from the identification algorithm.

Table 2. Statistics of daily averaged modal frequencies

Mode No.	Maximum (Hz)	Minimum (Hz)	Average (Hz)	Relative variation (%)
1	0.1237	0.1233	0.1235	0.3244
2	0.1806	0.1792	0.1797	0.7813
3	0.2808	0.2780	0.2790	1.0072
4	0.3441	0.3391	0.3408	1.4745
5	0.3832	0.3752	0.3784	2.1322
6	0.4588	0.4511	0.4536	1.7069

A polynomial regression model is further applied herein for the modeling of frequency-temperature seasonal correlations. The seasonal correlations can be mathematically described as

$$f(T,n)=p_nT^n+p_{n-1}T^{n-1}+\cdots+p_2T^2+p_1T^1+p_0 \quad (1)$$

where T is the daily averaged value of temperature; f is the daily averaged values of the frequency; n is the order

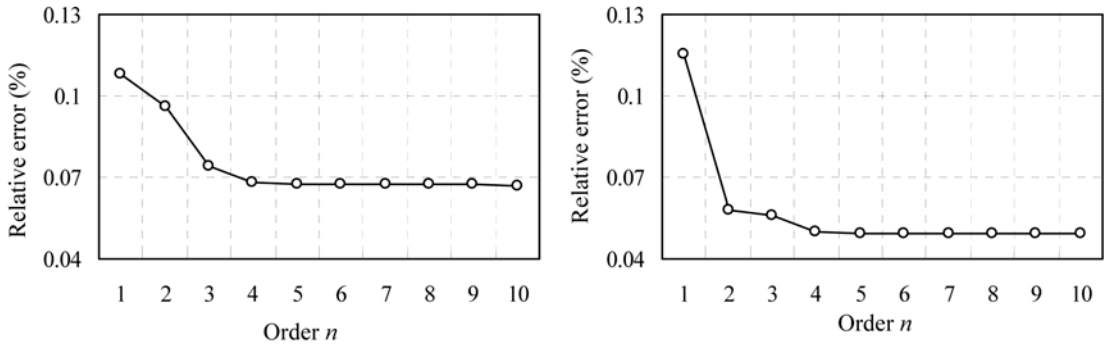

Figure 10. Mean values of relative errors between the measured and predicted frequencies.

Table 3. Summary of polynomial regression models

Mode	Regression function (f: frequency (Hz); T: temperature (°C))
1	$f(T)=1.1285\times10^{-12}T^6-2.7442\times10^{-10}T^5+1.6987\times10^{-8}T^4-3.8560\times10^{-7}T^3+2.8113\times10^{-6}T^2-7.9556\times10^{-6}T+0.1237$
2	$f(T)=6.6960\times10^{-12}T^6-7.3456\times10^{-10}T^5+2.5466\times10^{-8}T^4-2.3168\times10^{-7}T^3-2.3921\times10^{-6}T^2+3.4614\times10^{-6}T+0.1802$
3	$f(T)=3.6489\times10^{-12}T^6-5.8201\times10^{-10}T^5+2.7526\times10^{-8}T^4-4.3476\times10^{-7}T^3+1.4373\times10^{-6}T^2-7.4533\times10^{-5}T+0.2804$
4	$f(T)=8.5268\times10^{-12}T^6-1.3241\times10^{-9}T^5+6.3712\times10^{-8}T^4-1.0614\times10^{-6}T^3+3.6787\times10^{-6}T^2-1.3557\times10^{-4}T+0.3435$
5	$f(T)=-1.5680\times10^{-12}T^6+1.5204\times10^{-10}T^5-1.8955\times10^{-8}T^4+1.4321\times10^{-6}T^3-4.1850\times10^{-5}T^2+1.8027\times10^{-4}T+0.3822$
6	$f(T)=2.6275\times10^{-11}T^6-3.2575\times10^{-9}T^5+1.3731\times10^{-7}T^4-2.0896\times10^{-6}T^3+5.5445\times10^{-6}T^2-2.0162\times10^{-4}T+0.4581$

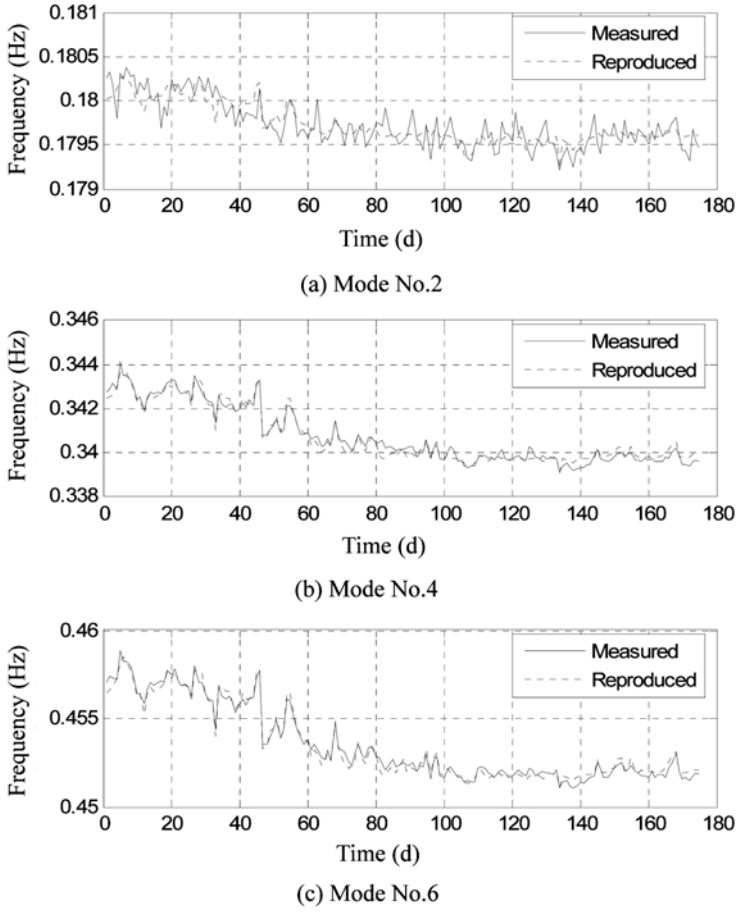

Figure 11. Comparisons of the measured and polynomial reproduction results of frequencies.

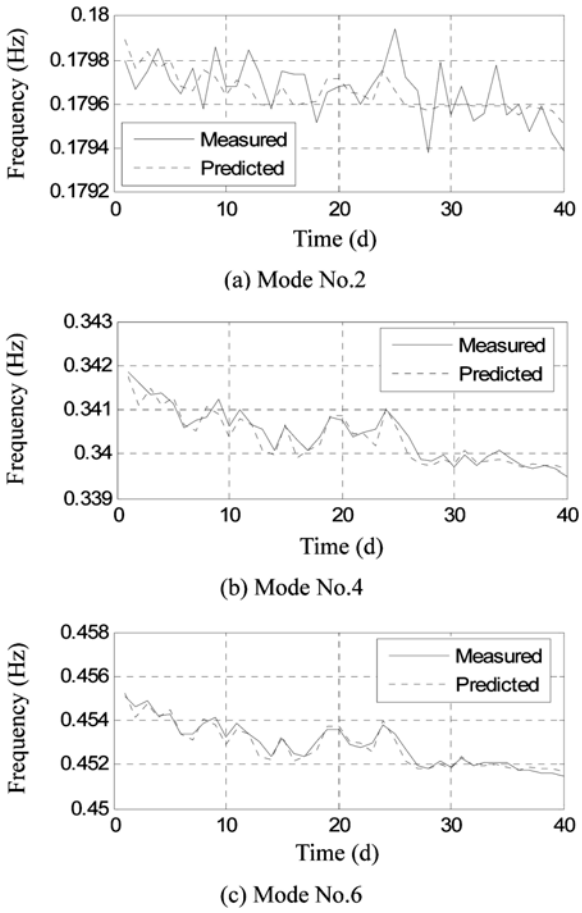

Figure 12. Comparisons of the measured and polynomial predicted results of frequencies.

of polynomial regression model; $p_i(i=0\sim n)$ is the coefficient of the regression model.

The 175-day monitoring data are discontinuously extracted from the total 215-day data for training the model and the other 40-day monitoring data are used for testing the prediction capability. Firstly the order n of the regression model is selected to achieve the optimal prediction capabilities. By increasing the number of n from 1 to 10, the regression models are formulated using 175-day training data and the relative errors of measured and predicted frequencies can be obtained. Figure 10 shows the mean values of relative errors between the measured and predicted frequencies for 175-day training data for different vibration modes. It can be seen that the when the number of n is increased from one to four, the mean value has a dramatic reduction. Then the mean value has insignificant changes with the increase of the number of the order n. Finally, the order n of the regression model is set to 6 in this study. Table 3 summarizes the expressions of polynomial regression functions. Figure 9 shows the curve regressed using the polynomial regression models of frequency-temperature. Figure 11 shows the comparisons of the measured and polynomial reproduction results using 175-day training data. The reproduction values of modal frequency favorably agree with the measured values, which indicate the satisfactory reproduction capability of the regression model.

Then the 40-day temperature data are fed into the trained regression model to generate the prediction values of modal frequency which are compared with the measured values to evaluate the prediction capability. As shown in Fig. 12, the predicted values of modal frequency favorably agree with the measured values, which indicate the satisfactory prediction capability of the regression model. On the whole, the developed polynomial regression model exhibits good capabilities for mapping between the temperature and measured modal frequency so that the temperature-caused variability of the modal frequency can be effectively quantified.

4.3. Removal of temperature effect

Before the measured frequencies are used for structural health monitoring, the temperature effect on the measured modal frequencies should be removed. It is achieved by normalizing all the measured frequencies to a fixed reference temperature with the use of the established seasonal correlation models. In this study, the reference temperature is taken as 20°C. By presenting the reference temperature into the correlation models, a nominal frequency (f_r) is obtained for each vibration mode. Likewise, by feeding the daily averaged temperature into the model, a temperature induced frequency (f_t) is predicted. Then the normalized frequency after removing temperature effect can be obtained by

$$f=f_m-(f_t-f_r) \tag{2}$$

where f is the normalized modal frequency; f_m is the daily averaged modal frequency. Figure 13 show the daily averaged and normalized modal frequencies for the Runyang Suspension Bridge.

Table 4 provides the statistics of the normalized modal frequencies. By comparing the relative variations shown in Table 4 with those given in Table 2, it is concluded that the temperature effect on the daily averaged frequencies can be effectively removed. The maximum and averaged relative variations for Runyang Suspension Bridge reduced from 2.1322 and 1.2377% to 0.5573 and 0.3992%. Thus, seasonal correlation models of frequency-temperature can effectively eliminate the temperature effect and random variations rising from the identification algorithm and it is suitable for on-line structural health monitoring and damage warning.

5. Conclusions

In this paper the temperature-induced variations of measured modal frequencies of steel box girder for Runyang Suspension Bridge have been studied based on long-term continuous measurement data. The following are the findings and conclusions.

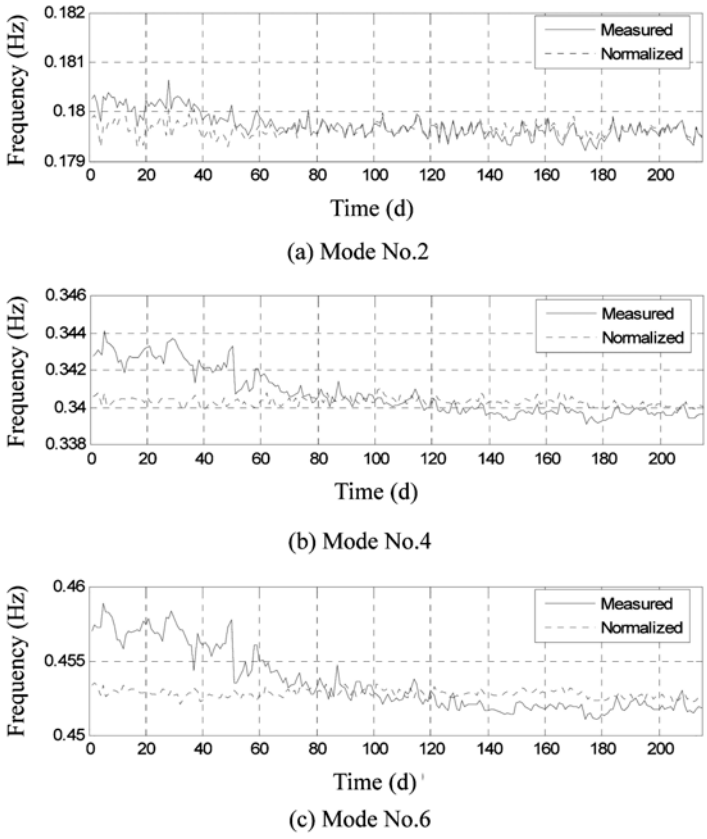

Figure 13. Daily averaged and normalized modal frequencies.

(1) The output-only modal frequency identification of the long-span suspension bridges has been effectively carried out using the Iterative Windowed Curve-fitting Method (IWCM) to overcome the shortcomings of limited frequency resolutions in the frequency-domain. The identified modal frequencies using IWCM provide an effective indication for changes of the bridge due to the ambient temperature variations.

(2) From the daily correlations of temperature-frequency, it can be observed that an overall decrease in modal frequency is observed with the increase in temperature of the bridge and measured modal frequencies of higher vibration modes are more sensitive to ambient temperatures. However, the frequency-temperature scatter diagrams are too dispersed to be an effective description of the correlation of frequency-temperature because of the random variations rising from the identification algorithm.

(3) The daily averaged modal frequencies of vibration modes have remarkable seasonal correlations with the daily averaged temperature, implying that the random variations rising from the identification algorithm can be effectively eliminated. A polynomial regression model is further applied for the modeling of daily averaged frequency-temperature and temperature-caused variations of the modal frequency can then be effectively quantified.

(4) Based on the seasonal correlation models of frequency-temperature, the temperature effect and random variations rising from the identification algorithm can be effectively eliminated. Thus, it is suitable for structural damage warning if future seasonal correlation models deviate from these normal models.

Table 4. Statistics of normalized modal frequencies

Mode No.	Maximum (Hz)	Minimum (Hz)	Average (Hz)	Relative variation (%)
1	0.1238	0.1233	0.1235	0.4055
2	0.1801	0.1793	0.1796	0.4462
3	0.2793	0.2784	0.2788	0.3233
4	0.3411	0.3399	0.3403	0.3530
5	0.3789	0.3768	0.3779	0.5573
6	0.4535	0.4521	0.4528	0.3097

Acknowledgments

The authors wish to acknowledge the support of the National Natural Science Foundation of China (No. 50725828, No. 50808041 and No. 50978056), Ph.D. Programs Foundation of Ministry of Education of China (No. 200802861011), Teaching and Research Foundation for Excellent Young Teacher of Southeast University.

References

Abdel Wahab, M. and De Roeck, G. (1997). "Effect of temperature on dynamic system parameters of a highway bridge." *Structural Engineering International*, 7(4), pp. 266-270.

Cornwell, P., Farrar, C. R., Doebling, S. W., and Shoh, H. (1999). "Environmental variability of modal properties." *Experimental Techniques*, 23(6), pp. 45-48.

Ding, Y. L., Li, A. Q., and Liu, T. (2008a). "Environmental variability study on the measured responses of Runyang Cable-stayed Bridge using wavelet packet analysis." *Science in China Series E: Technological Sciences*, 51(5), pp. 517-528.

Ding, Y. L., Li, A. Q., Sun, J., and Deng, Y. (2008b). "Experimental and analytical studies on static and dynamic characteristics of steel box girder for Runyang Cable-stayed Bridge." *Advances in Structural Engineering*, 11(4), pp. 425-438.

Doebling, S. W., Farrar, C. R., and Prim, M. B. (1998). "A summary review of vibration-based damage identification methods." *Shock and Vibration Digest*, 30(2), pp. 91-105.

Han, S. H., Cho, H. N., Cho, T. J., Shin, S. W., and Kim, T. S. (2010). "Risk assessments of long-span bridges considering life-cycle cost concept and near-fault ground motion effect." *International Journal of Steel Structures*, 10(1), pp. 51-63.

Hsieh, K. H., Halling, M. W., and Barr, P. J. (2006). "Overview of vibrational structural health monitoring with representative case studies." *Journal of Bridge Engineering*, 11(6), pp. 707-715.

Hua, X. G., Ni, Y. Q., Ko, J. M., and Wong, K. Y. (2007). "Modeling of temperature-frequency correlation using combined principal component analysis and support vector regression technique." *Journal of Computing in Civil Engineering*, 21(2), pp. 122-135.

Ko, J. M. and Ni, Y. Q. (2005). "Technology developments in structural health monitoring of large-scale bridges." *Engineering Structures*, 27(12), pp. 1715-1725.

Lee, J. W., Choi, K. H., and Huh, Y. C. (2010). "Damage detection method for large structures using static and dynamic strain data from distributed fiber optic sensor." *International Journal of Steel Structures*, 10(1), pp. 91-97.

Macdonald, J. H. G. (2000). *Identification of the dynamic behaviour of a cable-stayed bridge from full-scale testing during and after construction.* Ph. D. thesis, University of Bristol, UK.

Ni, Y. Q., Hua, X. G., Fan, K. Q., and Ko, J. M. (2005). "Correlating modal properties with temperature using long-term monitoring data and support vector machine technique." *Engineering Structures*, 27(12), pp. 1762-1773.

Ni, Y. Q., Ko, J. M., Hua, X. G., and Zhou, H. F. (2007). "Variability of measured modal frequencies of a cable-stayed bridge under different wind conditions." *Smart Structures and Systems*, 3(3), pp. 341-356.

Ni, Y. Q., Zhou, H. F., and Ko, J. M. (2009). "Generalization capability of neural network models for temperature-frequency correlation using monitoring data." *Journal of Structural Engineering*, ASCE, 135(10) pp. 1290-1300.

Peeters, B. and De Roeck, G. (2001). "One-year monitoring of the Z24-Bridge: environmental effects versus damage events." *Earthquake Engineering and Structural Dynamics*, 30(2), pp. 149-171.

Ren, W. X. and Peng, X. L. (2005). "Baseline finite element modeling of a large span cable-stayed bridge through field ambient vibration tests." *Computers and Structures*, 83(8-9), pp. 536-550.

Ren, W. X., Lin, Y. Q., and Peng, X. L. (2007). "Field load tests and numerical analysis on Qingzhou Cable-stayed Bridge." *Journal of Bridge Engineering,* ASCE, 12(2), pp. 261-270.

Sohn, H., Dzwonczyk, M., Straser, E. G., Kiremidjian, A. S., Law, K. H., and Meng, T. (1999). "An experimental study of temperature effect on modal parameters of the Alamos Canyon Bridge." *Earthquake Engineering and Structural Dynamics*, 28(8), pp. 879-897.

Zhang, Q. W., Fan, L. C., and Yuan, W. C. (2002). "Traffic-induced variability in dynamic properties of cable-stayed bridge." *Earthquake Engineering and Structural Dynamics*, 31(11), pp. 2015-2021.

Zhou, H. F., Ni, Y. Q., and Ko, J. M. (2010). "Constructing input to neural networks for modeling temperature-caused modal variability: Mean temperatures, effective temperatures, and principal components of temperatures." *Engineering Structures*, 32(6), pp. 1747-1759.